Monodomain ferroelectric region near the factory-roof-shaped phase front in the KD_2PO_4 218 K transition

2003 J. Phys.: Condens. Matter 15 4371

(http://iopscience.iop.org/0953-8984/15/25/308)

INSTITUTE OF PHYSICS PUBLISHING JOURNAL OF PHYSICS: CONDENSED MATTER

J. Phys.: Condens. Matter **15** (2003) 4371–4385 PII: S0953-8984(03)61133-1

Monodomain ferroelectric region near the factory-roof-shaped phase front in the KD_2PO_4 218 K transition

Jean Bornarel[1,3] **and Ryszard Cach**[2]

[1] Laboratoire de Spectrométrie Physique, Université Joseph Fourier, BP 87, 38402 Saint-Martin d'Hères Cedex, France
[2] Institute of Experimental Physics, University of Wroclaw, Pl M Borna 9, Pl-50-204 Wroclaw, Poland

E-mail: Jean.Bornarel@ujf-grenoble.fr

Received 20 March 2003
Published 13 June 2003
Online at stacks.iop.org/JPhysCM/15/4371

Abstract
Monodomain regions are observed in the uppermost ferroelectric parts of the factory-roof-shaped phase front during the KD_2PO_4 218 K first-order transition. It is also demonstrated that the existence of the phase front induces high values of dielectric and loss constants (along the *c* axis). An explanation is proposed assuming specific properties for the observed monodomain regions.

1. Introduction

KD_2PO_4 (DKDP) crystal, the deuterated isomorph of KH_2PO_4, undergoes a first-order transition between a tetragonal paraelectric and paraelastic phase ($\bar{4}2m$), which is the high-temperature phase, and an orthorhombic ferroelectric and ferroelastic one ($mm2$). The polarization P_z, which is considered as the order parameter, belongs to the B_2 representation as does the shear strain u_{xy} due to the piezoelectric behaviour of DKDP. Besides the shear strain appearance in the plane perpendicular to the ferroelectric axis *c*, can be noted the values of normal lattice deformation with $u_{zz} = 6.5 \times 10^{-4}$ greater than u_{xx} and u_{yy} (about 1×10^{-4}). In the low-temperature phase the ferroelectric–ferroelastic domain structure exists with permissible walls (Fousek and Janovec 1969) in (100) and (010) tetragonal planes. These domains are also mechanical twins and the importance of the mechanical energy in the domain structure of KDP-type crystals has long been known (Bornarel and Lajzerowicz 1968).

The first information about phase coexistence in DKDP came from the study of lattice deformations by neutron diffractometry (Zeyen and Meister 1976, Zeyen *et al* 1976). Intending to interpret the measurements, the authors suggested that paraelectric and ferroelectric stripes

[3] Author to whom any correspondence should be addressed.

perpendicular to the c ferroelectric axis alternate in the sample. The validity of this prediction was confirmed by direct optical observations (Bastie *et al* 1980) and by x-ray topography using synchrotron radiation (Aleshko-Ozhevskii 1982, 1983). As in these experiments the results were projections in a given direction, it was not possible to make conclusions about the shape of the phase front. More recently the phase coexistence of DKDP has been systematically studied. Observations along the three tetragonal axes were simultaneously performed, providing good results concerning the shape of the phase front (Bornarel and Cach 1991, 1993). The great importance of mechanical and chemical energy when the sample is under an external thermal gradient has been demonstrated: when external thermal gradient $\vec{G}_e$ is parallel to the ferroelectric c axis the phase front is quasiplanar and near the (001) plane (Bornarel and Cach 1994). When $\vec{G}_e$ is perpendicular to the c axis the phase front appears like a 'factory roof' the section of which in the a_1 (or a_2) tetragonal plane has a zigzag shape (Bornarel *et al* 1996a, 1996b). When the thermal gradient is small enough, for example 5×10^{-3} K mm^{-1} or less, only one or two quasiplanar phase fronts near the (001) plane take part in phase coexistence (Kvitek and Bornarel 1997, Bornarel and Cach 1999). A theoretical model explains these phenomena as due to competition between mechanical and chemical energies, with a quasi-negligible effect of the electrostatic energy at zero applied electric field (Kvitek 1997). The anisotropy of the mechanical energy is demonstrated with the help of Khachaturyan's theory (Khachaturyan 1983) where the work of elastic forces caused by the inclusion of an orthorhombic phase region inside an infinite crystal in the tetragonal phase is calculated. This explains the different shapes observed for the phase front in different situations for samples under $\vec{G}_e$ and without applied electric field. It has recently been demonstrated that contrary to many other examples of phase fronts (Dec 1993), the DKDP phase front is an incoherent interface (Kvitek and Bornarel 2002). The increase in the thermal hysteresis at the transition when a small dc electric field (or stress) is applied to the crystal is also explained (Kvitek and Bornarel 2000). The discrepancies in the literature between observations of thermal hysteresis equalling a few tenths of a degree kelvin (Strukov *et al* 1972) and thermal hysteresis below 10^{-2} K (Zeyen and Meister 1976) have been explained. The specific heat anomalies are also better understood (Strukov *et al* 1968). The shapes of the phase fronts in samples without an external field are understood on the whole, but a few questions remain. One of them is a possible correlation between the shape of the phase front and the domain texture. And more precisely, why has the ferroelectric region near the phase front sometimes been observed as monodomain and sometimes not? The purpose of the present paper is to answer this question for the case of phase coexistence with zigzag-shaped phase fronts. The experimental procedures allowing simultaneous observations along the three tetragonal axes and the dielectric measurements are described in the next section. Then the results section demonstrates the existence of monodomain regions near the ferroelectric ridges of the zigzag-shaped phase front and shows the correlation between the phase front, the appearance of the domain texture and the dielectric properties. These results are discussed in the last section where the contribution of the phase coexistence to the dielectric constant is calculated. Finally, it is suggested that the ferroelectric region is monodomain if its dimension d along c is smaller than a critical value d_c.

2. Experimental procedures

The DKDP crystals were grown by slow cooling in a supersaturated solution of KDP and heavy water. The deuteration was about 99%. The orientation of the sample faces, which were parallel to the tetragonal crystallographic planes, was verified with x-ray Bragg diffraction (accuracy of a minute of an arc).

The DKDP sample was set in a helium-gas exchange chamber of a cryostat allowing optical observations and measurements along three perpendicular axes simultaneously with dielectric measurements. These three axes were perpendicular to the sample faces. The observations along the a_i axes allow the shape of the phase front to be reconstructed, while the observations along the c axis give information about the domain texture, as illustrated in figure 1. The c ferroelectric axis corresponds to a horizontal optical axis. The thermal gradient $\bar{G}_e$ in the helium-gas chamber was vertical and monitored with an accuracy of 5×10^{-3} K mm^{-1} with the help of two platinum resistors placed just above and below the sample. The temperature reported later is that of the lower platinum resistor which was measured with a precision of 2×10^{-3} K. Each thermal cycle was performed as follows: the temperature was stabilized for several hours 1 °C above the temperature transition. The sample was cooled regularly during the paraelectric–ferroelectric (PF) cycles to 1 °C under the transition temperature (temperature rate equal 10^{-3} K min^{-1}). Then the temperature was decreased and the sample kept for 12 h at a temperature 15 °C under the transition temperature simplifying and stabilizing the domain structure. Finally the temperature was increased during the ferroelectric–paraelectric (FP) cycles at the same rates as during the cooling for the same temperature ranges. As previously demonstrated, it is possible to calculate the internal thermal gradient G_i experimentally by drawing the position of the phase front versus the measured temperature T (Bornarel *et al* 1996a, 1996b).

Two thin copper wires were glued with a spot of silver paste on the faces perpendicular to the c ferroelectric axis allowing the electrical contacts for dielectric measurements. The sample capacity and dissipation factor were measured using an HP 4274 A impedance meter with a measuring field of amplitude 1 V cm^{-1} and frequency 4 kHz, allowing ε_c' and ε_c'' to be calculated with a relative accuracy of 3×10^{-3} and 1×10^{-2} respectively. It is possible to simultaneously perform dielectric measurements, observation of the phase front and observation of the domain texture.

3. Results

The results concerning the phase front shape, the domain structure and the dielectric ε_c' and loss ε_c'' constants are presented in turn to make them clearer.

3.1. Phase front and domain texture

The results given in figures 1–4 correspond to DKDP sample A with dimensions $a_1 = 6.75$ mm, $a_2 = 3.85$ mm and $c = 4.98$ mm. Figure 1 illustrates the phase coexistence during a PF cycle under a thermal gradient $G_e = 0.81 \pm 0.07$ K mm^{-1}. The photographs show the phase front in an a_2 section (left) and the domain texture in a c section (right). The schematic illustration in figure 2 helps us understand the phenomenon. Daggers of ferroelectric phase appear first on the lower a_1 sample face which is the coolest (a). They are created in the centre of the face as well as in the corners and then overrun the whole of the a_1 face (b). The zigzag-shaped phase front leaves this a_1 face (c) and crosses the sample (d)–(f) to reach the upper a_1 sample face which is the hottest (g). Finally the paraelectric daggers disappear on this face. During the entire PF cycle, the domain texture phenomena can be described as follows: first of all, a dense and regular domain texture occurs only below the factory-roof-shaped phase front where the domains can cross the entire sample in the c direction. In the ferroelectric region, only the permissible wall (Fousek and Janovec 1969, Sapriel 1975) perpendicular to $\bar{G}_e$ usually exists (parallel to the (100) plane in figures 1 and 2). On the contrary, the two different domain species can be observed inside the ferroelectric daggers of the factory-roof

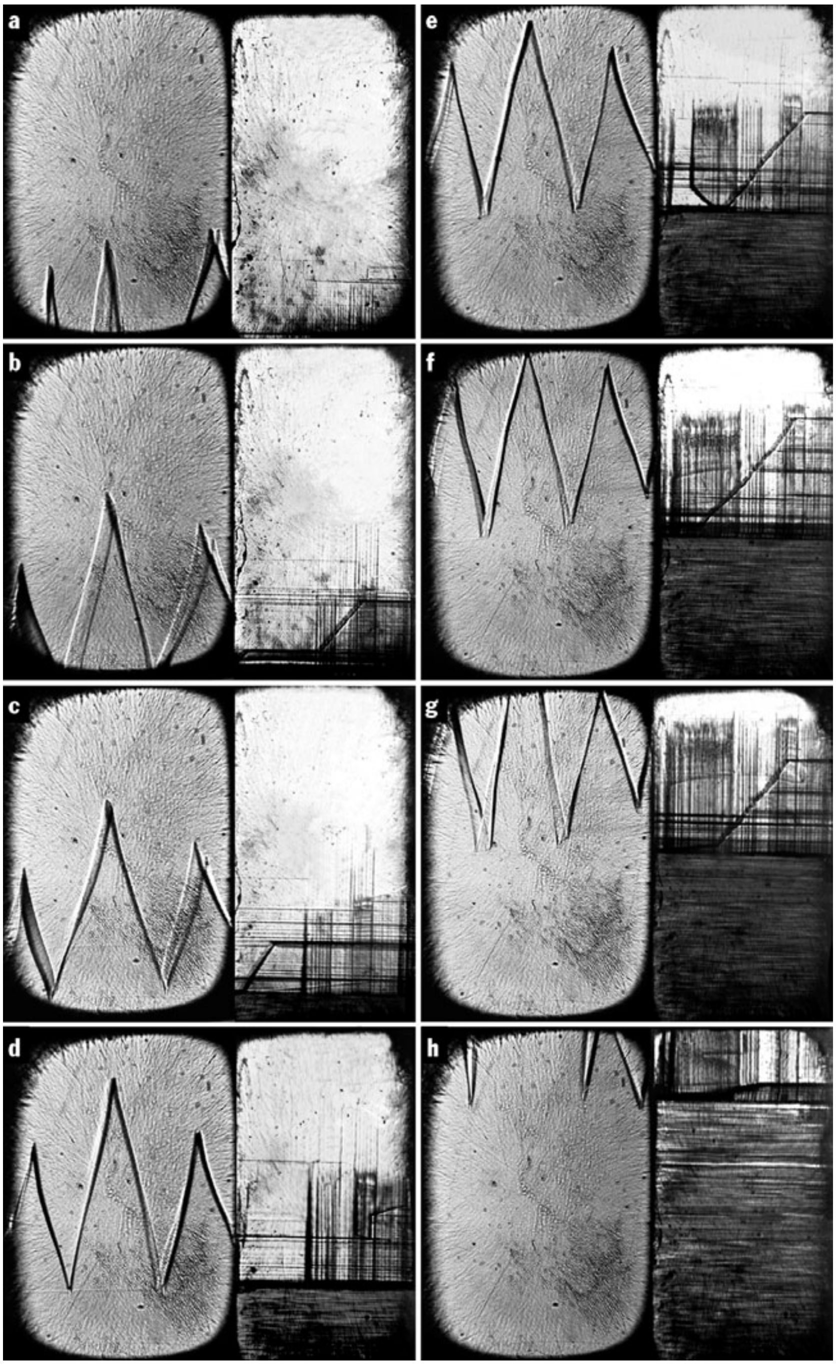

Figure 1. Photographs of the phase front in an a_2 section (left) and of the domain texture in a c section (right) during a PF cycle (sample A, $G_e = 0.81 \pm 0.07$ K mm^{-1}).

region. Sometimes continuous processes in the domain texture are observed, in other cases abrupt domain rearrangements occur inducing modifications like waves in all the ferroelectric regions of the sample as well. The domains are very unstable inside the daggers and all

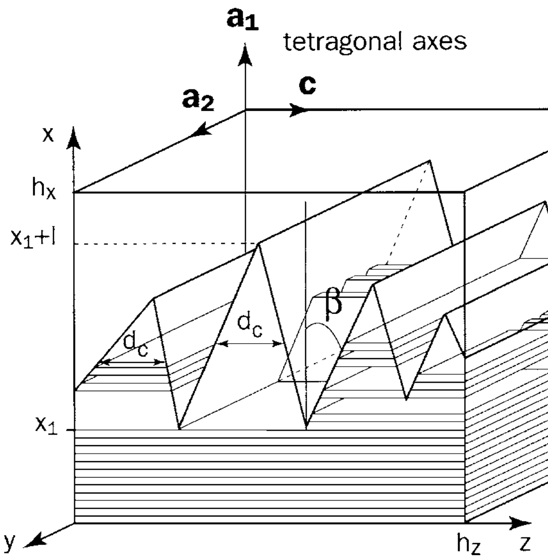

Figure 2. Schematic representation of the zigzag-shaped phase front and of the domain texture. When the phase fronts are nearer than d_c the ferroelectric region is like a monodomain.

these modifications lead to boundaries between domain species in planes (010), (110) or $(1\bar{1}0)$ as illustrated in figure 1. Another important phenomenon is the monodomain state of the uppermost part of the ferroelectric daggers: when the distance along c between two phase fronts is smaller than a critical value d_c, no domain is observed. During the PF cycle shown in figure 1, $d_c = 720 \pm 220\ \mu$m. To clarify this result, the FP cycle is performed with a smaller G_e value ($G_e = 0.74 \pm 0.02$ K mm^{-1}) with the purpose of obtaining only one dagger. Figure 3 illustrates this situation. First, contrary to the PF case, the domain texture remains stable during the entire FP cycle where the phase front sweeps away the domains. The domain texture is dense and regular below the factory-roof-shaped phase front region. Through the dagger, the domain texture is clearer but this could be due to the thinner twinned region crossed by the light along c. But the upper part of the dagger appears monodomain like, as in the PF case. The critical value d_c here equals $d_c = 550 \pm 100\ \mu$m.

3.2. Dielectric properties

The observations in sample B ($a_1 = 6.66$ mm, $a_2 = 4.41$ mm and $c = 7.11$ mm) allow us to correlate phase front, domain texture variations and dielectric measurements. The internal gradient was calculated and found to be equal to 0.109 ± 0.03 K mm^{-1}. In figures 4 and 5 the two peaks in the $\varepsilon_c'(T)$ curve, at the beginning and the end of the PF curve correspond to the hooking up of the daggers (P or F) on an a_1 sample face. These maximum values of ε' (15 000) are clearly higher than during the motion of the factory-roof-shaped phase front across the sample (ε_c' between 11 000 and 12 000).

The $\varepsilon_c''(T)$ variation exhibits a large peak (12 000) at the beginning of the PF cycle with a quasiconstant value (4000) everywhere else. The phenomena described in figure 1 are also observed here: instability of the domain texture, very mobile domains in the daggers and monodomain regions near their upper ridges (with $d_c = 650 \pm 130\ \mu$m). Furthermore, the phase front shape is different in the bulk of the sample and near the a_1 faces: the angles β

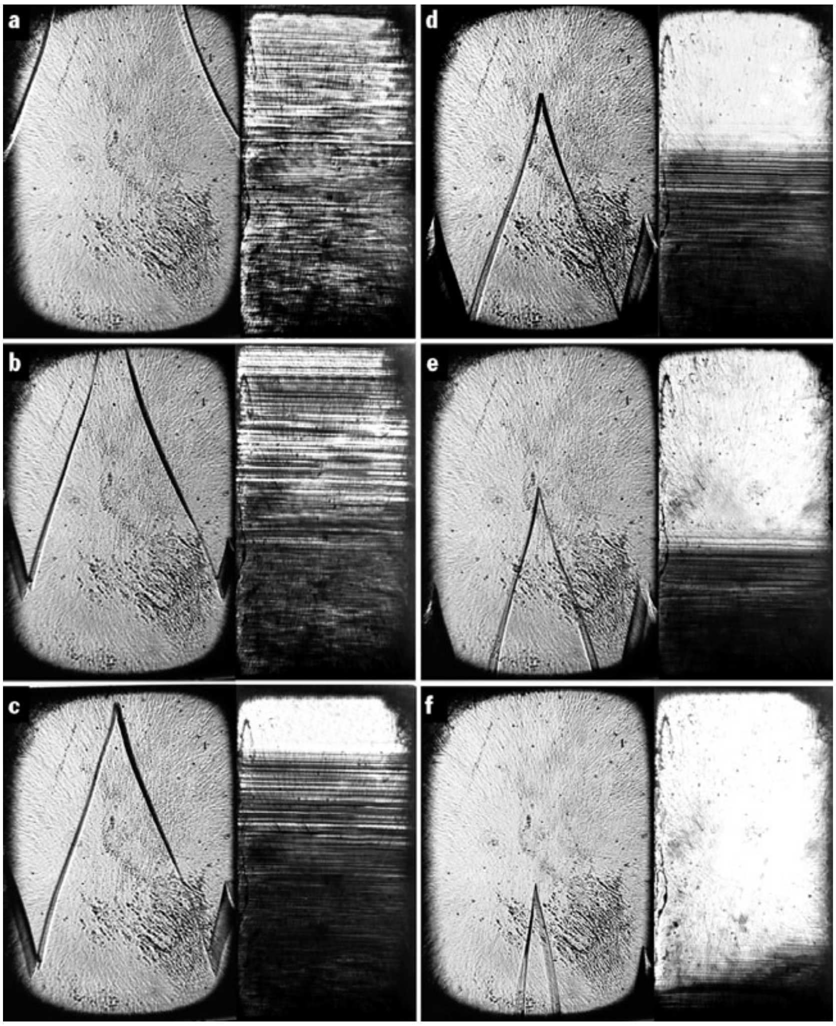

Figure 3. Photographs of the phase front in an a_2 section (left) and of the domain texture in a c section (right) during an FP cycle (sample A, $G_e = 0.74 \pm 0.02$ K mm^{-1}).

between a phase front part and the (001) plane look regular in the bulk; they change when the ridges of the daggers are hooked on the sample boundaries. The distortion of the daggers is also easy to see.

The FP cycle in sample B was performed under a G_i value equal to 0.076 ± 0.003 K mm^{-1}. Photographs of the phase front and domain texture, and the temperature variation of ε_c' and ε_c'' are presented in figures 6 and 7 respectively. It is possible to note that the domain texture remains stable and is swept away by the phase front. Furthermore the monodomain state in the upper parts of the ferroelectric daggers is confirmed (with $d_c = 550 \pm 60$ μm). The ε_c' and ε_c'' values remain quasiconstant during the FP cycle and always below the ones for the PF cycle at similar temperatures, as noted in previous papers.

The purpose of the present paper is not to study the zigzag shape of the phase front (in an a_2 section) in detail but its variation as illustrated by the β distribution in figure 8. All the β values regularly measured during PF and FP cycles are plotted. The smaller values

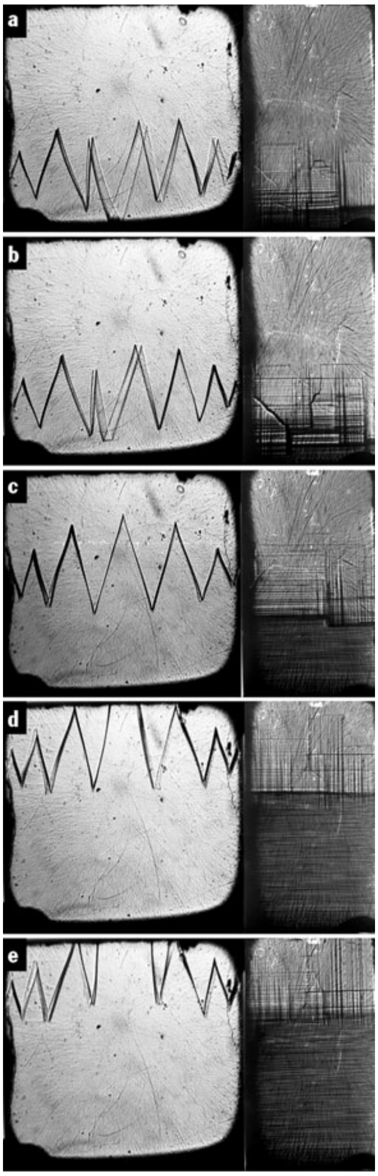

Figure 4. Photographs of the phase front in an a_2 section (left) and of the domain texture in a c section (right) during a PF cycle (sample B, $G_i = 0.109 \pm 0.03$ K mm^{-1}).

around 14–15 degrees of arc correspond to phase front parts hooked to a_1 sample boundaries. The higher values around 20–21 degrees of arc correspond to parts hooked to the c sample boundaries and the intermediate values (16–19 degrees of arc) to phase front parts in the bulk of the sample. These values are only weakly dependent on the G_i value as demonstrated in a recent paper (Kvitek and Bornarel 2002).

4. Discussion

The above results provide information on the shape of the phase front and on the domain texture during DKDP transitions when the sample is under a thermal gradient $\bar{G}_e$ perpendicular to

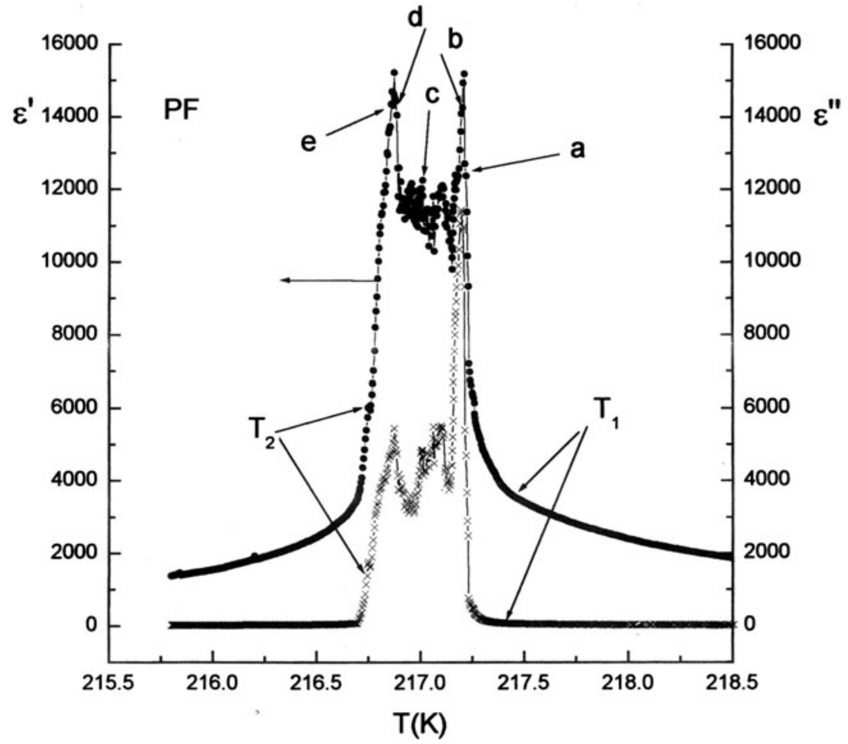

Figure 5. Temperature variation of the dielectric constant ε'_c and of the loss constant ε''_c during the PF cycle illustrated in figure 4. The letters correspond to the part labels in figure 4.

the c axis. The phase front appears factory-roof-shaped. It seems that under G_i of similar magnitude, the number of dagger ridges is greater during PF cycles than during FP ones. This needs to be verified with accurate measurements of the internal gradient G_i as a function of the rate of change of temperature (Bornarel *et al* 1996a, 1996b) The most important result concerns the existence of monodomain regions near the phase front. During PF cycles, a dense domain texture appears only below the coexistence region, in the ferroelectric phase where the domains can cross the whole sample along the c direction. The ferroelectric daggers of the phase coexistence region are almost monodomain with only a few unstable and mobile domains inside. On the contrary, during FP cycles a dense and stable domain texture already exists before the start of the transition. The appearance of the phase front does not induce rearrangements in the domain texture which is only scanned by the front. Only the uppermost parts of the ferroelectric daggers are observed as monodomain when the distance between the phase front parts is smaller than $d_c = 550 \pm 60\ \mu$m. These results clarify previous observations in which monodomain states in the coexistence region were sometimes noted and sometimes not. The fact that the phenomena are different during heating and cooling cycles is consistent with previous works. For example, it is well known that domain textures change a few degrees below T_C during cooling cycles but not during heating ones. These fluctuations and rearrangements explain the higher values for the dielectric constant during cooling cycles in comparison with heating cycles (Nakamura *et al* 1984, Bornarel 1987). Similarly, it has been demonstrated with short-circuited and isolated KDP samples under applied shear stress that appearance and disappearance of domains is more easily obtained with a decreasing temperature rate than an increasing one (Bornarel *et al* 1972).

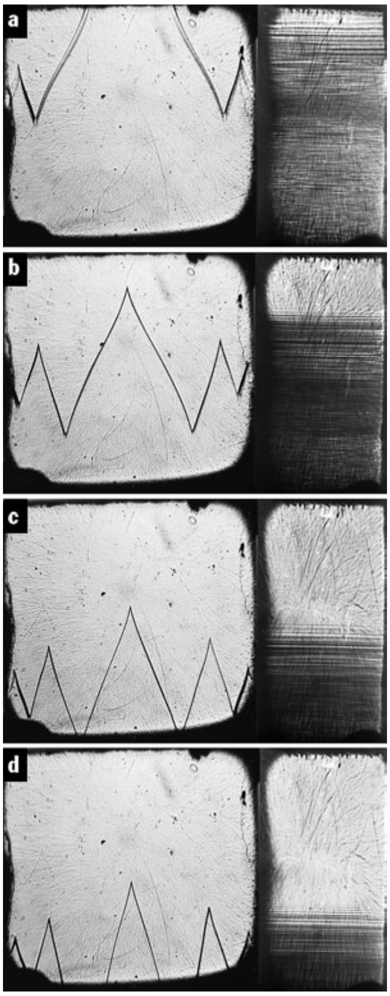

Figure 6. Photographs of the phase front in an a_2 section (left) and of the domain texture (right) during an FP cycle (sample B, $G_i = 0.076 \pm 0.003$ K mm^{-1}).

The fact that d_c is smaller during FP cycles than during PF ones is consistent with all these results. The value $d_c = 550\ \mu$m($\pm 100\ \mu$m) is the lowest observed in our experimental conditions. Different models are envisaged to explain the existence of the monodomain region and will be the subject of another paper. The widening of the domain walls near the transition (Andrews and Cowley 1986) is correlated with a narrow domain width whose observation would become optically impossible. This hypothesis seems excluded due to the very clean polydomain region boundary in the FP cycle case. It has also been considered that phase fronts play the same role as sample boundaries in surface layers (Sekido and Mitsui 1967, Chincholkar and Unruh 1968) and in small KDP particles (Jaccard *et al* 1953). But taking into account recent works, particular attention is devoted to the mechanical energy due to the phase front. In this case models with long-range forces as studied first by Khachaturyan and Roitburd (Roitburd 1984, 1993) and adapted recently to DKDP crystals (Kvitek 1997), are not sufficient because they concern infinite samples. A promising way is to consider the effect of the uniaxial pressure created by the jump in u_{zz} which becomes stronger as d becomes smaller.

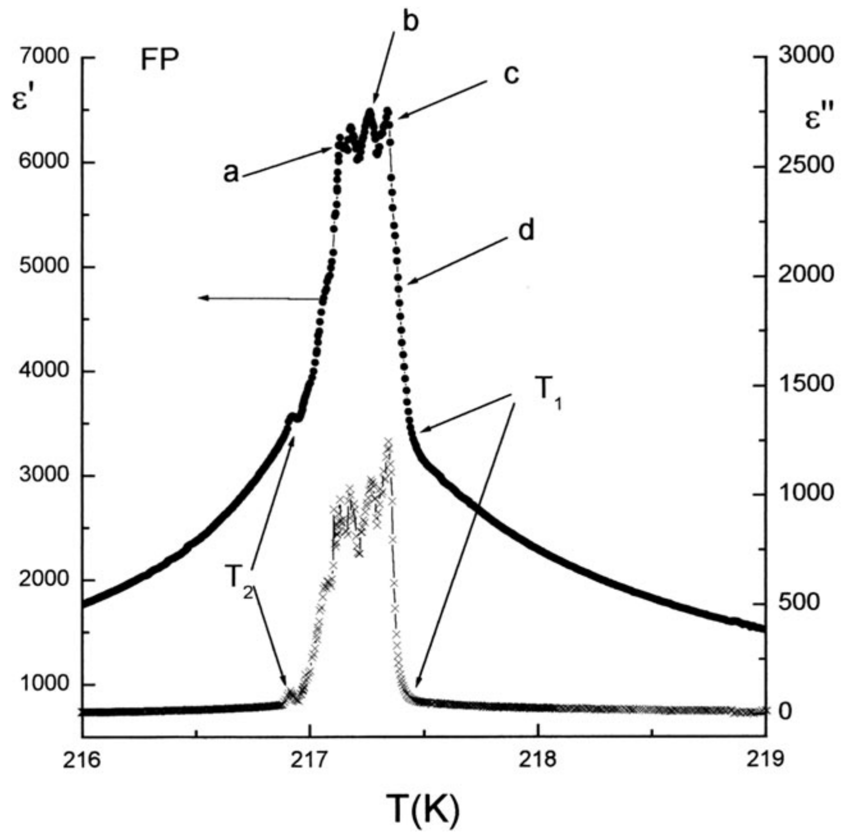

Figure 7. Temperature variation of ε_c' and ε_c'' during the FP cycle illustrated in figure 6. The letters correspond to the part labels in figure 6.

The importance of such stress on the transition temperature and on the dielectric properties has recently been studied (Stasyuk *et al* 1999) as well as the effect of a shear stress (Stasyuk *et al* 2000) following many papers on the effects of hydrostatic pressure effects (Blinc and Zeks 1968, Samara 1979, Hikita *et al* 1992). Complementary experiments are performed with samples under very small thermal gradients to investigate these hypotheses. The purpose is to determine if the lines of singularity, i.e. the ridges of the daggers, play a role or not: if two parallel planar phase fronts are nearer than d_c, is the ferroelectric volume between them monodomain? First results seem to give an affirmative answer (Bornarel and Cach 1999) but more conclusive observations are in progress.

We shall now correlate our observations with the dielectric properties. Firstly, the loss constant ε_c'' is observed to have very small values outside the phase coexistence region (in figures 5 and 7). On the contrary, during phase coexistence the ε_{PC}'' value is equal to 4250 ± 1250 for the PF cycle (except for the peak at the beginning of the transition) and 800 ± 300 for the FP cycle. The peak at the beginning of the PF cycle corresponds to the creation of the dense domain texture below the phase coexistence region: for the first time the domains cross the entire sample, which corresponds to moving charges and rearrangements. Even if the phenomenon is not known in detail, the fact that it induces abrupt modifications in losses is understandable. Except for this event, ε_{PC}'' values are relatively constant during a cycle and these values can be correlated to the volumes in the coexistence region corresponding to

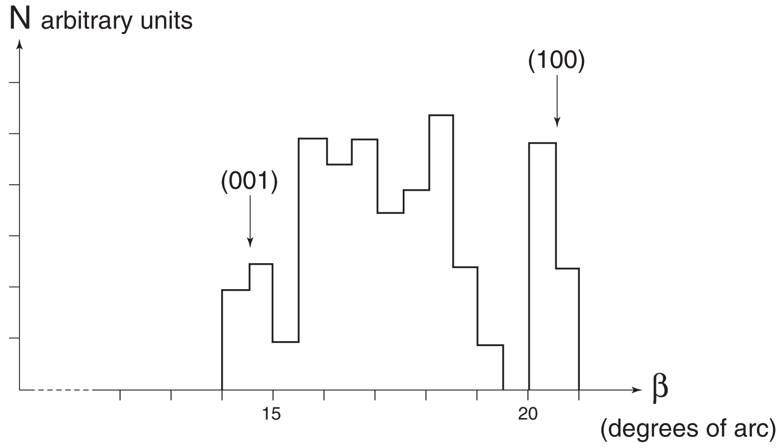

Figure 8. Distribution of the β angle values during PF and FP cycles. The smallest and biggest values correspond to phase fronts hooked on the sample boundaries c and a_1 respectively.

monodomain ferroelectric parts. For example the dimension e of this 'monodomain' region in the a_1 direction is 2.8 ± 0.2 mm during the PF cycle (the height of all the daggers in figure 5) and 1.05 ± 0.2 mm during the FP cycle (figure 7). The large uncertainties reported above are not due to the measurement of e or to the sample dimension along a_1 but to the different interpretations of this parameter: the lower values correspond to real monodomain regions and the higher to regions in which the domain texture is not dense or stable. It is possible to see that the greater the value of e is, the greater is ε''_{PC}, even if the ratio between PF and FP values does not produce the same result (5.3 ± 2 for ε''_{PC} and 2.8 ± 0.7 for e). If all the ε''_{PC} values are considered to be due to the 'monodomain' region of the phase coexistence, the local value of ε''_c varies between 5000 (FP) and 10 000 (PF), which is very high (the equivalent resistance at 4 kHz is 2.6×10^5 and 1.4×10^6 Ω respectively). This global estimation demonstrates the high conductivity of the phase coexistence region where the ferroelectric part is monodomain.

It is possible to use models already described in previous work (Bornarel *et al* 1996a, 1996b) to analyse the ε'_c results. Firstly, the temperature $T'(x)$ inside the sample can be considered to be linearly dependent on the position x along a_1 and the problem can be studied in the (010) plane:

$$T(x) = T + \frac{x}{h_x}\Delta T \tag{1}$$

where ΔT is the difference between temperatures of the highest and of the lowest a_1 sample faces, and h_x is the sample dimension along the a_1 direction. Furthermore, the isotherm at the Curie temperature T_C is taken in the middle of the phase coexistence region. The validity of hypothesis (1) has already been experimentally demonstrated (Bornarel *et al* 1996a, 1996b). The capacitance C measured between the c electrodes can be considered to be made up of parallel capacitances:

$$C = \frac{h_y\varepsilon}{h_z}\left[\int_0^{x_1} \varepsilon'_F(x)\,\mathrm{d}x + \int_{x_1}^{x_1+e} \varepsilon'_{PC}(x)\,\mathrm{d}x + \int_{x_1+e}^{h_x} \varepsilon'_P(x)\,\mathrm{d}x\right] \tag{2}$$

where h_y and h_z are the sample dimensions in the a_2 and c directions respectively, x_1 is the coordinate in x of the boundary between the ferroelectric region and the phase coexistence region of dimension e, ε'_F, ε'_P and ε'_{PC} are the dielectric constants in the ferroelectric region, in the paraelectric region and in the phase coexistence region respectively.

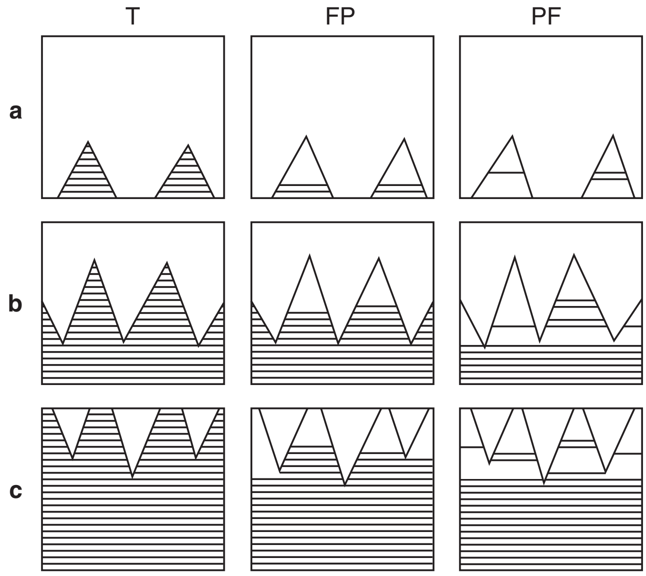

Figure 9. Schematic representations in the a_2 section of the phase front and of the domains. Drawings to the left correspond to the hypothesis of the presented model and the others are similar to the experimental observations during PF (right) and FP (middle) cycles.

ε'_P follows the Curie–Weiss law, experimentally verified:

$$\varepsilon'_P(T) = \frac{C_P}{T - T_0} \tag{3}$$

with C_P and T_0 equal during the PF cycle (figure 5) to 4572 and 216.87 K respectively, and during the FP cycle (figure 6) to 4418 and 217.12 K respectively (the measured temperature T is the lower platinum resistor one, which explains the difference between the T_0 values). The dielectric constant of the ferroelectric region has been shown to be the sum of the contribution due to the monodomain ε'_m and to the domain existence ε'_d (Bornarel and Cach 1999).

ε'_m can be calculated with C_P, T_0 and the value of the second coefficient B of the Landau development of the free energy (using $B = 4.5 \times 10^{10}$ SI obtained by Sidnenko and Gladkii). It has also been experimentally shown (Bornarel and Cach 1999) that ε'_d is proportional to ε'_m with a factor depending on the domain density. The usual logarithmic variation versus T can be approximated near the transition by:

$$\varepsilon'_F(T) = \varepsilon'_m + \varepsilon'_d = \frac{C_F}{T_1 - T} \tag{4}$$

with C_F and T_1 equal during the PF cycle to 2211 and 218.05 K respectively, and during the FP cycle to 3248 and 218.9 K.

To calculate the second integral of the relation (2), the hypothesis illustrated in figure 9 (left) is adopted: the ferroelectric region in the phase coexistence is considered as polydomain with a regular domain texture which allows us to employ relations (3) and (4) and

$$\varepsilon'_{PC}(z, \varepsilon'_P, \varepsilon'_F) = \left[\frac{1}{\varepsilon'_F} + \left(\frac{1}{\varepsilon'_P} - \frac{1}{\varepsilon'_F}\right)\frac{z}{h_z}\right]^{-1} \tag{5}$$

where z, for a given coordinate x, is the part of the h_z dimension of the sample (along the c direction) occupied by the paraelectric phase. It is possible to calculate the second integral

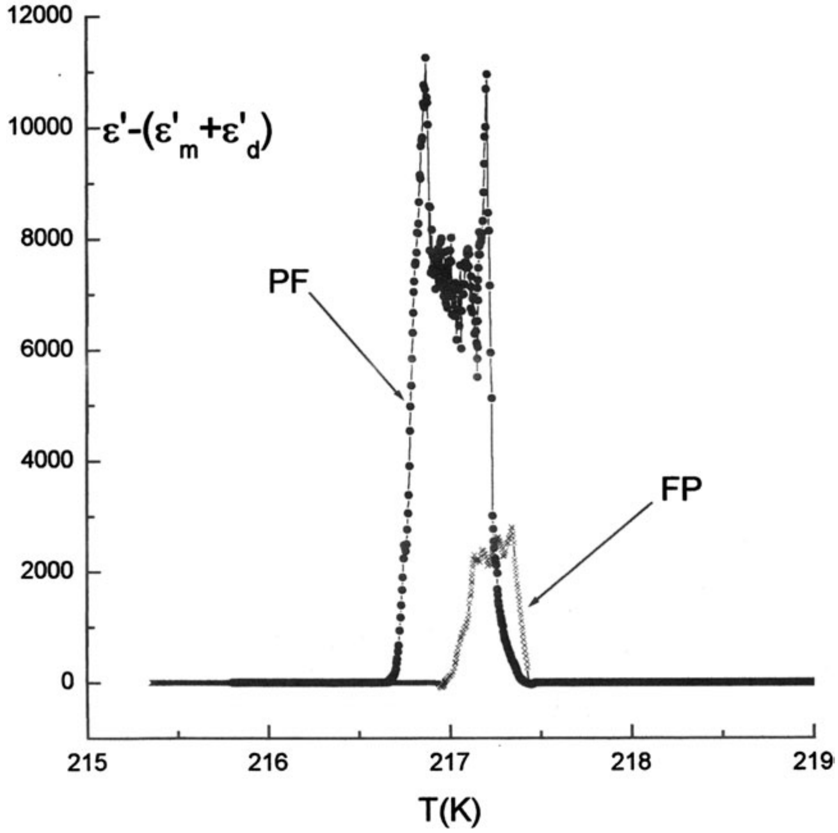

Figure 10. Temperature variation of the contribution to the dielectric constant due to the existence of a phase front.

inside the brackets of (2) using relation (1) for the temperature variation versus x, or adopting the hypothesis that the temperature is constant and equals T_C in the phase coexistence region. The results for these two cases are not very different: 13.8 and 15.1 m in the PF cycle. After that we compare the value of the measured dielectric constant ε' to the one calculated as previously explained. The difference, called $\varepsilon' - (\varepsilon'_m + \varepsilon'_d)$, is shown in figure 10. The peaks in the PF curve at the beginning and at the end of the phase coexistence can be attributed to the appearance (and disappearance) of the phase front inducing many domain arrangements, which is not easy to model. On the contrary, it is possible to compare the previous model illustrated in figure 9 (left) with the observations. During the FP cycle, $\varepsilon' - (\varepsilon'_m + \varepsilon'_d) = 2500 \pm 300$ and the uppermost parts of the daggers are monodomain as illustrated in figure 9 (middle), with a value of the local dielectric constant different from $\varepsilon'_m + \varepsilon'_d$. During the PF cycle, $\varepsilon' - (\varepsilon'_m + \varepsilon'_d) = 7000 \pm 500$ as shown in figure 9 (right). If the local dielectric constant in the monodomain dagger parts for a given x coordinate is called ε_1 we can write

$$\varepsilon' - (\varepsilon'_m + \varepsilon'_d) = \frac{1}{h_x} \int_b^{x_1+e} [\varepsilon'_{PC}(z, \varepsilon'_p, \varepsilon_1) - \varepsilon'_{PC}(z, \varepsilon'_p, \varepsilon'_F)]\, \mathrm{d}x \tag{6}$$

where b is the lower limit of the domain region. In the PF case (where $b = x_1$), the resolution of equation (6) with all the coexistence phase supposed to be at temperature T_C, produces a value of 6.35×10^5 for ε_1, which is a high but plausible value. The resolution of (6) is not so evident in the FP case where this simple hypothesis is not sufficient. The limits of our modelling are reached and more information is needed on the correlation between the monodomain volume in the daggers and the local dielectric properties in the ferroelectric region as well as in the paraelectric one. For this reason we are now studying the correlation between the calculated values $\varepsilon' - (\varepsilon'_m + \varepsilon'_d)$ and the monodomain or quasimonodomain volume in the phase coexistence region. When G_i is very small, all the sample can be involved (Bornarel and Cach 1999); on the contrary, when G_i is very high or parallel to c, there is no monodomain region. This study is still in progress and will be published later. All other models involving small vibrations of the phase front, charge space effects, etc will also be explored.

5. Conclusion

The existence of monodomain ferroelectric regions during DKDP phase coexistence which exhibit factory-roof-shaped phase fronts has been experimentally demonstrated. During a PF cycle all the ferroelectric daggers are involved, but only their uppermost parts are involved during an FP cycle. In the presented results the ferroelectric region is monodomain where the distance between the phase fronts is less than $550 \pm 60\ \mu$m. Further experiments are necessary to confirm the existence of this critical distance d_c and to explain it. Furthermore, during phase coexistence the dielectric constant and the losses are not only the sum of contributions due to the monodomain sample and to the domains. The contributions due to the phase coexistence are very important in the macroscopic measurements: up to 4000 for ε''_c and 11 000 for ε'_c. For the first time some explanations have been proposed depending on the importance of the monodomain region. One possibility is the existence of regions with very high dielectric and loss constant values. Further studies of situations with differently shaped phase fronts are required.

References

Aleshko-Ozhevskii O P 1982 *Sov. Phys.–Crystallogr.* **27** 673
Aleshko-Ozhevskii O P 1983 *Ferroelectrics* **48** 157
Andrews S R and Cowley R A 1986 *J. Phys. C: Solid State Phys.* **19** 615
Bastie P, Bornarel J, Dolino G and Vallade M 1980 *Ferroelectrics* **26** 789
Blinc R and Zeks B 1968 *Helv. Phys. Acta* **41** 701
Bornarel J 1987 *Ferroelectrics* **71** 255
Bornarel J and Cach R 1991 *Ferroelectrics* **124** 345
Bornarel J and Cach R 1993 *J. Phys.: Condens. Matter* **5** 2977
Bornarel J and Cach R 1994 *J. Phys.: Condens. Matter* **6** 1663
Bornarel J and Cach R 1999 *Phys. Rev.* **60** 3806
Bornarel J, Cach R and Kvitek Z 1996a *J. Phys.: Condens. Matter* **8** 7365
Bornarel J, Cach R and Kvitek Z 1996b *J. Phys.: Condens. Matter* **8** 11327
Bornarel J, Fousek J and Glogarova M 1972 *Czech. J. Phys.* B **22** 864
Bornarel J and Lajzerowicz J 1968 *J. Appl. Phys.* **39** 4339
Chincholkar V S and Unruh H G 1968 *Phys. Status Solidi* **29** 669
Dec J 1993 *Phase Transit.* **45** 35
Fousek J and Janovec V 1969 *J. Appl. Phys.* **40** 135
Hikita T, Ono Y and Bungo A 1992 *J. Phys. Soc. Japan* **61** 3794
Jaccard C, Känzig W and Peter M 1953 *Helv. Phys. Acta* **26** 521
Khachaturyan A G 1983 *Theory of Structural Transformation in Solids* (New York: Wiley–Interscience)
Kvitek Z 1997 *J. Phys.: Condens. Matter* **9** 127
Kvitek Z and Bornarel J 1997 *Ferroelectrics* **190** 31
Kvitek Z and Bornarel J 2000 *J. Phys.: Condens. Matter* **12** 7819
Kvitek Z and Bornarel J 2002 *Eur. Phys. J.* B **30** 153
Nakamura E, Ushio S and Abe K 1984 *J. Phys. Soc. Japan* **53** 403

Roitburd A L 1984 *Sov. Phys.–Solid State* **26** 1229
Roitburd A L 1993 *Phase Transit.* **45** 1
Samara G A 1979 *Ferroelectrics* **22** 925
Sapriel J 1975 *Phys. Rev.* B **12** 5128
Sekido and Mitsui T 1967 *J. Phys. Chem. Solids* **28** 967
Sidnenko E V and Gladkii V V 1973 *Sov. Phys.–Crystallaogr.* **17** 861
Stasyuk I V, Levitskii R R and Moina A P 1999 *Phys. Rev.* B **59** 8530
Stasyuk I V, Levitskii R R, Zachek I R and Moina A P 2000 *Phys. Rev.* B **62** 6198
Strukov B A, Amin M and Kopchik V A 1968 *Phys. Status Solidi* **27** 741
Strukov B A, Baddur A and Velichko I A 1972 *Sov. Phys. Solid State* V **13** 2085
Zeyen C M E and Meister H 1976 *Ferroelectrics* **14** 731
Zeyen C M E, Meister H and Kley W 1976 *Solid State Commun.* **18** 621